Journal of Superconductivity, Vol. 10, No. 5, 1997

Coupling Across an Intimate Cuprate–Manganite Interface

W. E. Pickett[1,2]

Received 1 July 1997

Electronic and magnetic coupling across the interface between a ferromagnetic $La_{2-x}Ba_xMnO_4$ ("colossal magnetoresistance" CMR) layer and a $La_{1.85}Ba_{0.15}CuO_4$ (high-temperature superconductor) layer are studied in a self-consistent virtual crystal approximation using the local spin density functional approach. The manganite material dopes the first cuprate layer, with holes if $x=2/3$ and with electrons if $x=0$. For x near the CMR regime the ferromagnetic manganite slab should be half-metallic. Such multilayer systems may be useful as magnetic field-controlled current switches, or as a relatively high-temperature superconducting material with small critical field.

KEY WORDS: $La_{2-x}Ba_xMnO_4$; colossal magnetoresistance; $La_{1.85}Ba_{0.15}CuO_4$; high-temperature superconductor interface.

1. INTRODUCTION

Layering of ferromagnetic (FM) and superconducting (SC) materials is a growing research activity. From the point of view of the magnetic properties, there are basic questions such as whether a superconducting layer will affect magnetic coupling in a sandwich structure differently than a normal metal layer does, or how the onset of superconductivity affects the magnetic properties of the system as a whole. Solutions of the Bogoliubov–de Gennes equations by Sipr and Györffy [1] indicate that magnetic coupling is destroyed by a superconducting layer with thickness of the order of the superconducting coherence length. From the superconductivity viewpoint, the effect of magnetic spacing layers may result in novel vortex motion and cause unusual field and voltage dependences of electronic transport. On another level, magnetic/superconducting superlattices provide a larger-scale realization of certain magnetic superconducting compounds (viz. $RBa_2Cu_3O_3$, $RRhB_4$, RMo_6S_8, where R is a rare earth ion) [2] in which magnetism is confined to a region of the cell that is avoided by the conduction electrons. In addition, proximity of FM and superconducting materials can lead to new phenomena, such as the predicted "π-phase" [3] in which the superconducting order parameter alternates in sign in layers separated by magnetic spacer layers.

Recent explorations indeed reveal some aspects of the coupling between magnetic and superconducting layers. Studies of V/Fe multilayers [4] and Nb/Gd/Nb trilayers [5] have begun to reveal the dependence of the superconducting critical temperature, T_c, and the critical field depends on the thickness of the FM spacer layer. Mattson *et al.* [6] report that an 11 Å FM layer is sufficient to decouple SC layers in Fe_4N/NbN multilayers. A more complex example is the $DyBa_2Cu_3O_7/Sr_{1-x}Ca_xRuO_3$ multilayer system, where Miéville *et al.* [7] have determined how the vortex dynamics in the superconductor changes as the thickness of the FM layers are varied.

In this paper we address a related system, but at the atomic level. The concern here is not the effect of superconductivity on magnetic ordering or of magnetism on superconducting coupling, but the atom-level issue of charge and spin transfer across at most a few atomic layers. Representative members of the high-temperature superconducting (HTS) cuprates and the "colossal magnetoresistance" (CMR) manganites are chosen, both because they are highly interesting materials and also because they should be chemically and

[1]Complex Systems Theory Branch, Naval Research Laboratory, Washington DC 20375.
[2]Current address: Department of Physics, University of California, Davis, CA 95616.

0896-1107/97/1000-0577$12.50/0

structurally compatible. Excellent thin films of both kinds of materials can be grown through vapor phase techniques [8], and work on systems such as those treated here have already begun [9].

2. STRUCTURE OF SUPERLATTICE

For the cuprate slab of our model superlattice we choose the La_2CuO_4 (La214) structure. Although there is more experimental work on the YBCO-type HTS, and La-based manganites have already been grown on $Bi_2Sr_2CaCu_2O_{8+\delta}$ [9], these cuprates present undesirable complications for an initial study including (a) orthorhombic rather than tetragonal structure, (b) almost twice as many atoms per cell, and (c) for YBCO there is no natural (001) cleavage plane so any chosen structure would be more tentative. In the La214 (K_2NiF_4) structure [10] the conventional primitive cell consists of disjoint, neutral [LaO–CuO_2–LaO] slabs that provide a realistic candidate for the cuprate part of the cell.

The next question is how to connect this slab to a manganite slab with the perovskite structure. The lattice constants are a good match, with each being near 3.9 Å. One possibility is to use the LaO layer of the La214 structure also as an LaO layer in the perovskite structure, which has the layer stacking sequence [$\cdots$LaO–$MnO_2\cdots$]. With such a choice this charged LaO layer will contribute to doping in both of the adjacent CuO_2 and MnO_2 layers. Since we wish to try to "dope" our individual HTS and CMR layers by known amounts, we have not chosen this stacking sequence.

Instead we choose for the manganite slab three layers of the perovskite stacking sequence [LaO–MnO_2–LaO], which has the same stoichiometry (and structure) as our La214 slab. The resulting structure is shown in Fig. 1. A thicker slab of this type could be constructed by inserting additional LaO–MnO_2 bilayers, eventually building up a peroskite material terminated by LaO planes on each side. The various possibilities of constructing an interface geometry, two of which have been mentioned here, are indicative of complications that will arise in actual interface growth.

We choose the doping level we want to consider by using a "virtual crystal" (VC) approach. In the VC approximation, we replace La atoms (nuclear charge $Z=57$) with averaged La–Ba atoms with the desired average charge. In the calculations the nucleus can be assigned the corresponding nonintegral charge, and then the electronic and magnetic structure is determined self-consistently as usual. For the HTS slab we choose the virtual atom $Lb \equiv 0.925\ La + 0.075\ Ba$ ($Z=56.925$), corresponding to a VC treatment of the optimally doped (for superconductivity at $T_c=30$ K) $La_{2-x}Ba_xCuO_4$, $x=0.15$. For the manganite slab we want to dope the Mn ion to the level comparable to that in the CMR manganite perovskites, $Mn^{+3\frac{1}{3}}$. For our slab this requires the VC atom $Lm \equiv \frac{1}{3}La + \frac{2}{3}Ba$ ($Z=56\frac{2}{3}$). Thus our superlattice is $Lc_2CuO_4/Lm_2\ MnO_4$. (Notation: Lc indicates La-derived VC atom in the Cu slab; Lm indicates La-derived VC atom in the Mn slab.)

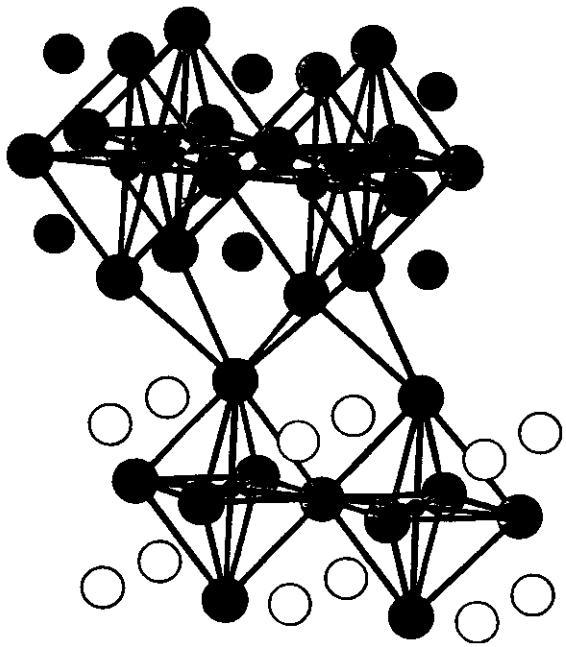

Fig. 1. Structure of the superlattice, based on the K_2NiF_4 structure.

We refer to this model HTS/CMR superlattice as SL1. In addition, we have studied another case in which the doping level of the Mn ions is different. In this superlattice SL2, we use actual La atoms in the manganite slab, i.e., La_2MnO_4, which corresponds to adding $1\frac{1}{3}$ electrons to this slab, giving a nominal Mn^{2+} ion corresponding to (possibly unreasonably) large doping of the Mn ion. This change in carrier density allows some estimation of the possibility of charge transfer across the interface (between MnO_2 and CuO_2 layers).

3. METHOD OF CALCULATION

We use the full potential linearized augmented planewave (LAPW) method [11–13] with calculational procedures giving well-converged one-electron

orbitals and densities [14]. The sphere radii were 2.20 for La, Lm, and Lc ions, 1.90 for the Cu and Mn ions, and 1.55 for oxygen, all in a.u. Local orbitals were used to help represent semicore states, so all calculations were done within a single energy window. The basis consisted of 1700 LAPWs and local orbitals, and self-consistency was carried out on a six special point mesh in the irreducible Brillouin zone.

For our structure we have used the lattice constants $a = 3.89$ Å and $c/a = 3.49$, consistent with unit cell sizes in La214 and with the perovskite lattice constant in the manganites. The internal positions of all of the atoms outside the Mn and Cu layers were relaxed until the energy was minimized for SL1. The resulting values of z/c were 0.1368 for Lm, 0.1686 for O_{Lm} (the oxygen in the Lm layer), 0.3572 for O_{Lc}, and 0.3300 for Lc. From the various energies it is possible to extract the four Raman active A_g phonons, whose frequencies were found to be: 94 cm^{-1} (larger Lc displacement than Lm displacement, some oxygen), 165 cm^{-1} (larger Lm displacement than Lc, some oxygen), 278 cm^{-1} (mostly O_{Lm} character, some Lm contribution), and 422 cm^{-1} (mostly O_{Lc} character, some Lm and Lc contribution). Since the structure and the masses are quite similar in the HTS and CMR portions of the structure, the lack of even approximate symmetry between these layers in the frequencies and the eigenvectors indicate that the forces involving these Mn and Cu ions are very different. To avoid complications in interpreting differences between the electronic and magnetic structures of SL1 and SL2, these same atomic positions were also used for SL2 rather than re-optimizing the structure for SL2.

4. SELF-CONSISTENT ELECTRONIC AND MAGNETIC STRUCTURE

In Fig. 2 we show the full density of states (DOS) for SL1 as well as the most important local DOS, those of Mn *d* and Cu *d* states. In Fig. 3 we focus on the *d* DOS near the Fermi level and compare SL1 and SL2. The 2*p* DOS for the various oxygen sites are presented in Fig. 4 Many of the important results can be identified from these figures.

We first focus on SL1. It is apparent from Fig. 2 that the ferromagnetism, as reflected in the spin splitting, is confined to the MnO_2 layer. The exchange splitting, identified from corresponding peaks in the majority and minority Mn *d* DOS, is 2.6 eV. This value is very close to what was obtained in bulk manganites at the same cell volume and similar Mn formal

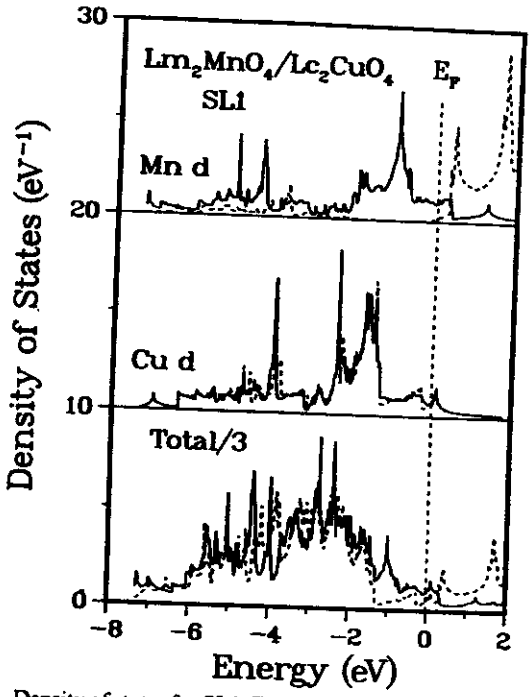

Fig. 2. Density of states for SL1. Top: Mn *d* local DOS, showing the spin splitting of 2.6 eV. Middle: Cu *d* local DOS, showing negligible spin polarization. Bottom: total DOS, illustrating that most of the oxygen DOS lies in the range −6 eV to −1 eV relative to E_F. Solid lines denote majority states; dashed lines are minority states.

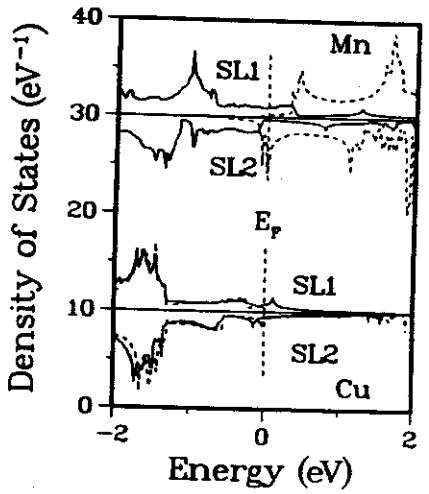

Fig. 3. 3*d* density of states near E_F (taken as the zero of energy) for both Mn and Cu in the superlattices. Solid lines show majority spin; dashed lines give minority spin. SL1 is plotted in the positive sense; SL2 is plotted in the negative sense. The alignment of the SL1 and SL2 Fermi levels in this figure has no physical significance.

charge [14]. There is negligible exchange splitting in the CuO_2 layer, indicating no induced magnetism even in the first Lc_2CuO_4 slab due to exchange splitting. (The macroscopic field will induce a moment proportional to the local susceptibility in the CuO_2 layer.)

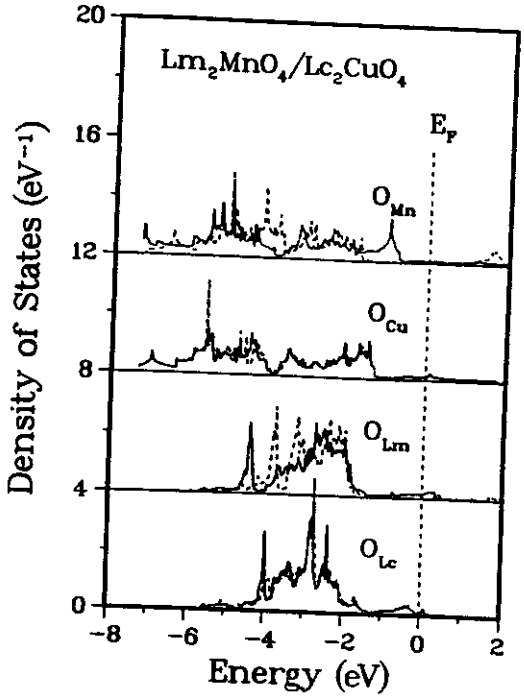

Fig. 4. Oxygen site densities of states for SL1. Solid (dashed) lines show majority (minority) states, with the largest polarization occurring on O_{Mn}.

The Cu $3d$ DOS is similar to its distribution in calculations for the bulk materials [10,15]. Note particularly the van Hove singularity (vHs) in the Cu DOS just above E_F. This vHs lies just at E_F at this filling in bulk $Lc_2CuO_4 \equiv La_{1.85}Ba_{0.15}CuO_4$. The shift of E_F away from the vHs peak indicates there is extra hole transfer (≈ 0.1) to the CuO_2 layer from the MnO_2 layer in SL1. Since there is no corresponding vHs in the Mn DOS, the wavefunction in the band that gives rise to this vHs is confined to the Lc_2CuO_4 slab, reflecting negligible coupling between the wavefunctions of the Fermi level carriers in the Mn and Cu parts of the cell.

As in the bulk system with the same Mn formal valence [14], there is a gap in the minority Mn channel between the O $2p$ states and the Mn $3d$ states. Such close similarity to the bulk spectrum is somewhat surprising, considering that this manganite layer is quite two dimensional while the bulk manganite is three dimensional. The Mn minority $3d$ band minimum lies 0.2 eV below E_F and forms a small pocket of electron carriers. We established earlier using supercell studies of $La_{2/3}Ca_{1/3}MnO_3$ that variations in the Mn $3d$ site energy $\delta\varepsilon_d \approx 0.5$ eV arise from the local cation charge variations (dipositive Ca vs. tripositive La). This strong site disorder is sufficient to localize the few minority carriers in the bulk. The disorder effect should be nearly identical in this SL1 system, since the concentration of divalent and trivalent ions is simply reversed. However, the magnetic system is two dimensional (2D) and, more to the point, the carrier transport is quasi-2D, for which defects have a greater localizing effect. Hence it seems likely that the Lm_2MnO_4 slab will be, for the purposes of transport, a 2D half-metallic ferromagnetic layer.

We now turn to the SL2 system. The additional $1\frac{1}{3}$ electrons in the cell go primarily into the MnO_2 layer, since that is the region of the cell that is near the increased nuclear charge (recall Lm with $Z = 56\frac{1}{3}$ in SL1 becomes La with $Z = 57$ in SL2). The charge (see the magnetic moments in Table I) goes almost equally into majority and minority states. As a result, the local Mn moment and the exchange splitting is unchanged from SL1. However, E_F is raised in the minority channel by an additional 0.5 eV into a region of large DOS, so the half-metallic character will no longer be present, that is, both spins will contribute strongly to transport. The added charge in the manganite layer dopes the CuO_2 layer somewhat and induces a magnetic moment of at least $0.1\mu_B$ on the Cu ion.

The local DOS of the SL1 system are shown in Fig. 4. The most noticeable distinction is between the O ions in the metal layers (O_{Mn} and O_{Cu}) and the out-of-layer O ions. The layer oxygens form extended 2D complexes with the neighboring d states, leading to the spread of spectral density over 7 eV or more. This is absent in the O_{Lm} and O_{Lc} ions, and most of their states are confined to a 3 eV region. The local DOS of the various oxygen sites of SL2 (not shown) indicates a Madelung shift downward of the O_{La} site by 1.5 eV in going from Lb to La, while other O sites are nearly unaffected. This shift decreases the Mn–O_{La} hybridization, which will tend to enhance the 2D character of the electronic structure in the La_2MnO_4 layer.

Table I. Spin Moments within the LAPW Spheres on Atoms in the Two Superlattices SL1 and SL2, Illustrating the Direction and Amount of Spin Transfer upon Adding Majority Charge to the MnO_2 layer

Atom	SL1	SL2
Mn	3.11	3.11
O_{Mn}	0.10	0.07
O_{Lb}	0.02	0.05
O_{Lc}	—	—
O_{Cu}	0.00	0.002
Cu	−0.004	0.09

Dispersion of the cuprate and manganite derived bands within the $\hat{a}$–$\hat{b}$ plane is comparable to that in the respective bulk materials. Dispersion along the $\hat{c}$ axis is sensitive to the coupling between layers. For bands near E_F we find dispersions of majority bands in the SL1 system in the range 0.06–0.16 eV, which correspond to effective transfer integrals in the range $t_\uparrow \approx 30$–80 meV. For the minority band just below E_F the corresponding value is $t_\downarrow \approx 15$ meV, which probably reflects the decreased hybridization of minority Mn d states with O p states [14]. The question of whether these values are large enough to give coherent transport along the $\hat{c}$ axis is moot, however, because the scattering due to the large cation disorder ($La^{3+}Ba^{2+}$) will almost certainly lead to incoherent $\hat{c}$ axis transport.

5. DISCUSSION AND SUMMARY

This initial study of intimate cuprate–manganite superlattices reveals the following characteristics. The ferromagnetic moment on the Mn ion is typical of the CMR manganites in spite of the single slab structure, no doubt reflecting the strong local character of the moment. The MnO_2 slab is effectively half-metallic, similar to the bulk manganite. For "optimally doped" cuprate and manganite layers, there is hole transfer from manganite to cuprate layers. A Ba-rich manganite slab will further hole-dope the nearest cuprate layer. For "optimally doped" cuprate and manganite layers, there is hole transfer from manganite to cuprate layers.

Only the ferromagnetic alignment of manganite slabs has been considered here. Due to the half-metallic nature of the manganite layer, in this FM multilayer charge transport along the $\hat{c}$ axis will be completely spin polarized, since minority tunneling between cuprate layers should be negligible. It is quite possible, perhaps even likely, that an antiferromagnetic ordering of manganite layers will be favored, but that the exchange coupling (which after all must proceed through the nonmagnetic cuprate layer) will be weak. If antiferromagnetism occurs, $\hat{c}$ axis transport will be cut off by the spin-valve effect of oppositely directed half-metallic layers [16]. Transport (polarized) can be restored by application of a magnetic field that aligns the moments in the manganite layers. Such a system would provide a field-controlled current switch.

Another unusual effect may occur when the multilayer system is superconducting. Multilayers with a single layer of the $YBa_2Cu_3O_7$ separated by as much as 70 Å of (insulating) $PrBa_2Cu_3O_7$ is superconducting [17], but for the Lc_2CuO_4 material studied here we are not aware of comparable experimental data. For antiferromagnetically aligned magnetic layers, the material might be superconducting—several cases are known where superconductivity coexists with antiferromagnetism in which the magnetic electrons are distinct from the superconducting electrons [2]. Application of a magnetic field large enough to align the manganite layers would lead to an antiferromagnetic-to-ferromagnetic transition that would suppress the superconductivity as well, due to the large internal magnetic field in the FM state. This sandwich structure provides a mechanism for suppressing superconductivity at fields well below the intrinsic critical field.

ACKNOWLEDGMENTS

I acknowledge helpful discussions with D. J. Singh and I. I. Mazin. This work was supported in part by the Office of Naval Research. Calculations were carried out at the Arctic Region Supercomputing Center and at the DoD Shared Resource Center at NAVO.

REFERENCES

1. O. Sipr and B. L. Györffy, *J. Phys.: Cond. Matter* **7**, 5239 (1995).
2. M. B. Maple, *Physica B* **215**, 110 (1995).
3. A. V. Andreev, A. I. Buzdin, and R. M. Osgood III, *Phys. Rev. B* **43**, 10124 (1991).
4. P. Koorevaar, Y. Suzuki, R. Coehoorn, and J. Aarts, *Phys. Rev. B* **49**, 441 (1994).
5. C. Strunk, C. Sürgers, U. Paschen, and H. v. Löhneysen, *Phys. Rev. B* **49**, 4053 (1994).
6. J. E. Mattson, C. D. Potter, M. J. Conover, C. H. Sowers, and S. D. Bader, *Phys. Rev. B* **55**, 70 (1997).
7. L. Miéville, E. Kollar, J.-M. Triscone, M. Decroux, O. Fischer, and E. J. Williams, *Phys. Rev. B* **54**, 9525 (1996).
8. I. Bozović and J. N. Eckstein, in *Physical Properties of High-Temperature Superconductors*, Vol. V, D. M. Ginsberg, ed. (World Scientific, Singapore, 1996).
9. I. Bozović and J. N. Eckstein, *Appl. Surf. Sci.* **113–114**, 189 (1997).
10. W. E. Pickett, *Rev. Mod. Phys.* **61**, 433 (1989).
11. O. K. Andersen, *Phys. Rev. B* **12**, 3060 (1975).
12. S. H. Wei and H. Krakauer, *Phys. Rev. Lett.* **55**, 1200 (1985); D. J. Singh, *Phys. Rev. B* **43**, 6388 (1991).
13. D. J. Singh, *Planewaves, Pseudopotentials, and the LAPW Method* (Kluwer Academic, Boston, 1994).
14. W. E. Pickett and D. J. Singh, *Phys. Rev. B* **53**, 1146 (1996).
15. W. E. Pickett, R. E. Cohen, and H. Krakauer, *Phys. Rev. Lett.* **67**, 228 (1991).
16. G. A. Prinz, *Phys. Today* **44**, No. 4, 58 (1995).
17. J.-M. Triscone, O. Fischer, O. Brunner, L. Antognazza, A. D. Kend, and M. G. Karkut, *Phys. Rev. Lett.* **64**, 804 (1990).